




Evaluating mechanical properties of duplex stainless steel with flux core arc welding: a comparison of welding modes

Viswanath Krishnan¹ , Anandavelu Kothandapany¹ , Pandiyarajan Rajendran² 

¹MRK Institute of Technology, Department of Mechanical Engineering, 608301, Kattumannarkoil, Tamilnadu, India.

²Agni College of Technology, Department of Mechatronics Engineering, 600130, Chennai, Tamilnadu, India.

e-mail: kviswanath@mrkit.in, anandavel01@yahoo.com, pandiyan.rajran8@gmail.com

ABSTRACT

This study investigates the mechanical properties of Flux Core Arc Welded (FCAW) Duplex Stainless Steel (DSS) under various welding modes: Constant Current (CC), Pulsed Current (PC), and Surface Tension Transfer (STT). Results indicate that the STT mode of FCAW delivers optimal mechanical properties, with yield strengths ranging from 711 MPa to 743 MPa and ultimate strengths from 758 MPa to 842 MPa. In comparison, CC mode yielded slightly lower results with yield strengths of 766 MPa to 781 MPa and ultimate strengths of 890 MPa to 901 MPa, while PC mode showed intermediate values. Impact strength analysis across CC, PC, and STT modes reveals that STT welds absorb the highest energy, ranging from 47 J to 48 J in the weld metal and 50 J to 74 J in the HAZ, compared to CC (20 J to 28 J) and PC (24 J to 38 J) modes. Fractographic analysis using Scanning Electron Microscopy (SEM) confirms uniform surface properties and minimal defects in STT mode welds, indicating improved weld integrity. Vickers hardness testing demonstrates higher values in the Heat Affected Zone (HAZ) near the weldment for STT mode (up to 300.27 HV), suggesting superior strength characteristics.

Keywords: Flux Core Arc Welding; Duplex Stainless Steels; Welding Modes; Mechanical Characterization.

1. INTRODUCTION

The Flux Cored Arc Welding (FCAW) process is optimal for outdoor or on-site fabrication due to its higher production of welding fumes compared to Gas Metal Arc Welding (GMAW). This excess of fumes effectively shields the weld metal, particularly in the fabrication of stainless steel [1, 2]. FCAW proves to be more economically viable than GMAW, especially when utilizing self-shielded flux-cored wires in on-site structural construction. The versatility of FCAW is further enhanced by the use of pulsed current (PC), which offers customizable settings that can be advantageous for various welding applications. Despite these advantages, there is a notable dearth of published literature on Duplex Stainless Steel (DSS) when utilizing FCAW [3, 4]. A primary concern in welding DSS is achieving a balanced (1:1) ratio of austenite to ferrite in the Weld Metal Zone (WMZ) and Heat Affected Zone (HAZ). This balance is critical for DSS joint fabrication and is influenced by filler metal chemistry, shielding gas, and heat input [5, 6]. Recent studies have highlighted that the use of pulsed current (PC) and Surface Tension Transfer (STT) mode of metal transfer provides superior control over heat input compared to Constant Current (CC) mode, which can lead to improved austenite–ferrite balance in the weld [7, 8]. One could expect better austenite–ferrite control in DSS joints if a PC and STT mode of metal transfer is used to join DSS base metal. However instead of using solid wire if one uses flux cored wire it will result in a productivity improvement compared to all other fusion welding processes about joining of DSS. So far, there is no pronounced research work focusing on the joining of DSS using PC and STT modes of metal transfers [9]. Thus, the two-fold benefit of Pulsed Current (PC)/Surface Tension Transfer (STT) and FCAW process needs to be explored for joining DSS in establishing austenite – ferrite balance in WMR in terms of Ferrite Number [10].

In the analysis of dissimilar welds between Incoloy 825 and UNS S32750 stainless steel, it was found that the weld metal exhibited textured properties with specific texture components, and grain growth and phase changes in the heat-affected zones (HAZs) led to increased texture intensities and reduced CSL boundaries compared to the base metals. CSL boundaries were absent in the weld metal [11]. Pulsed current (PC) was shown to increase ferrite content in Incoloy 825/UNS S32750 welds, which improved impact resistance. Incoloy 825 was identified as the weakest part of the welds, and the weld metals exhibited the weakest corrosion behavior at the

root pass. Overall, PC was found to enhance weld properties [12]. When comparing dissimilar welds of Incoloy 825 and SAF 2507 using different filler wires and welding techniques, it was observed that ERNiFeCr-1 filler produced a Ti-rich phase, while ER2594 created a Cr-rich phase. PCGTAW resulted in finer microstructures and lower ferrite content, with ERNiFeCr-1 and PCGTAW being recommended for better joint efficiency due to their improved hardness and toughness [13]. An assessment of microstructural features and texture evolution in welds between API X-65 steel and UNS S32750 stainless steel revealed that while the microtexture in UNS S32750 remained consistent, the texture in the API X-65 HAZ varied with heat input, affecting phase distribution. Lower heat input led to reduced austenite fractions, and weld metals showed better impact resistance compared to base metals [14]. The impact of electromagnetic vibration on the microstructure, mechanical properties, and hot-cracking susceptibility in 316L stainless steel welds demonstrated that electromagnetic vibration decreased columnar dendrites, increased hardness and toughness, and reduced hot-cracking susceptibility, with the fracture mode becoming more ductile at higher vibration voltages [15]. The use of continuous and pulsed current modes in dissimilar welds of AISI 316L and AISI 310S showed that pulsed current improved microhardness and impact toughness by refining dendrite structures and reducing unmixed zones. Fractures occurred on the 316L side, and austenite was the predominant phase in the weld metal [16]. Variations in pulse current settings in PCGTAW for AISI 316L-AISI 310S welds were found to affect the microstructure by reducing dendrite size and unmixed zone width, leading to enhanced hardness and fracture energy. Fracture occurred from the 316L side, with improved ductility and toughness [17]. The comparison of continuous vs. pulsed current in GTAW of AISI 316L stainless steel revealed that pulsed current led to finer grain structures, reduced unmixed zone width, and improved hardness and toughness, with the weld metal exhibiting an austenitic-ferritic microstructure and enhanced properties compared to continuous current welds [18]. Optimization of welding parameters for dual-phase steel DP600 and AISI 304 stainless steel using the Taguchi method identified current density, holding time, welding time, and electrode force as critical factors. The optimal conditions produced welds with martensitic structures and high tensile-shear strength [19]. The use of double-layer welding techniques for dissimilar materials showed improved joint quality with reduced microhardness in the heat-affected zone. The Higuchi and Modified Higuchi methods were tested with different electrodes, revealing that stress relief heat treatment was necessary for optimal results [20]. An investigation into how welding parameters affect the properties of nickel-based alloy coatings on ASTM A36 steel found that increased current led to greater dilution and changes in phase composition, which reduced hardness due to Fe diffusion from the substrate [21]. Nickel-based superalloy 625 weld overlays on carbon steel were assessed for mechanical and microstructural properties, showing satisfactory results in both as-welded and heat-treated conditions, including good hardness and bending properties [22]. The wear resistance of ASTM A242 steel welded with different filler metals was compared, revealing that wear resistance varied by region. The coarse grain heat-affected zone exhibited the highest resistance, with the filler metal's mechanical strength impacting the wear performance [23]. The study of how heat input and the number of layers affect duplex stainless steel weld deposits showed changes in chemical composition, microstructure, hardness, and pitting corrosion resistance with different heat inputs and layer numbers [24]. Analysis of weld beads from submerged arc welding using ultrasonic frequencies demonstrated that higher ultrasonic frequencies led to grain growth and improved impact toughness, with the energy absorbed during impact tests increasing with higher current and frequency [25]. Hard coatings applied via FCAW with Ti were found to have better wear resistance and fewer cracks compared to coatings without Ti, indicating that self-protected cored wire improves wear resistance [26]. In a microstructural evolution study of martensitic stainless steel 423Co used in continuous casting rolls under thermal fatigue, it was found that the coating showed martensitic slats and fine carbides that degraded with thermal fatigue, leading to material failure [27].

Despite the advances in FCAW processes and the benefits observed with pulsed current (PC) and Surface Tension Transfer (STT) modes, there remains a need to optimize these parameters specifically for joining Duplex Stainless Steel (DSS) plates. Existing research demonstrates various improvements in weld properties with PC and STT modes, but there is a lack of focused studies investigating their impact on DSS joints under optimized conditions. This study aims to address this gap by exploring the effects of different metal transfer modes on the mechanical and fractographical behavior of DSS joints, providing a comprehensive analysis of their performance under varying process parameters.

2. MATERIALS AND METHODS

2.1. Base metal: Duplex Stainless Steel 2205

The base metal for FCAW is ASTM S32205 (Trade name: SAF 2205[®]) Duplex Stainless Steel (DSS). This grade is selected as it is extensively applied in structural fabrication. The chemical compositions of the base metal and weld metal wire were determined by Energy Dispersive X-ray (EDX) analysis (Table 1).

Table 1: Chemical composition of base and weld metals.

MATERIAL	C	Mn	P	S	Si	Cr	Ni	Ti	Mo	Cu	N	Fe
Base metal: DSS (ASTM:S32205)	0.014	1.36	0.018	0.001	0.4	22.38	5.68	0.006	3.14	0.14	0.18	Balance
Weld metal: DSS Flux-cored Wire (AWS E2209T1-1/4)	0.03	1.2	0.002	0.001	0.07	23	9.2	–	3.1	0.1	0.12	Balance

**Figure 1:** Lincoln Electric Wave 455M/STT® power.

2.2. Experimental setup

Figure 1 displays the power source utilized in the chosen welding process (STT Lincoln Wave 455M). This system incorporates digitally controlled switches and systems, enabling precise control over maximum speed and waveform modes. In this research, three modes—CC, PC, and STT—are employed. The direction of the core wire is regulated by the welding gun using an automatic wire feeder mechanism. The results corresponding to each welding mode are promptly available, with digital data providing real-time readings.

Flux Cored Arc Welding (FCAW) demonstrates enhanced performance compared to other conventional fusion welding techniques for Duplex Stainless Steel (DSS) joints (Figures 2 and 3). FCAW is employed for joining DSS utilizing CC, PC, and STT modes. The welding parameters for each of these modes are outlined in Tables 2–4.

2.3. Characterization

The specimens for the tensile test were prepared as per ASTM E8M standard and tests were conducted on a computerized Universal Testing Machine (Machine Model: UT-40; Make: FIE). The test specimens were subjected to a rate of loading of 1.5 kN/min under standard test conditions, enough until the deformation of the specimens. The fracture behavior of the welded specimens was studied under the observations of the shock loading mechanics from the Charpy impact test and its subsequent energy absorption behavior. The Charpy v-notch specimen has dimensions of 55 × 10 mm with a notch of 2 mm depth along with a machined tip radius of about 0.25 mm on one face. To assess the strength of the weld joint, the Vickers microhardness testing machine is used. The surface of the sample is polished before this test either mechanically or by electrical means. The procedure followed to conduct this test is as per ASTM E384 standard. A diamond indenter was used to apply a range of load from 10 gf to 100 kgf at specific points on the surface of the weld joint in the specimen. For micro-hardness testing, the load is normally less than or equal to 1 kgf. The maximum time of indentation is 15 seconds and the

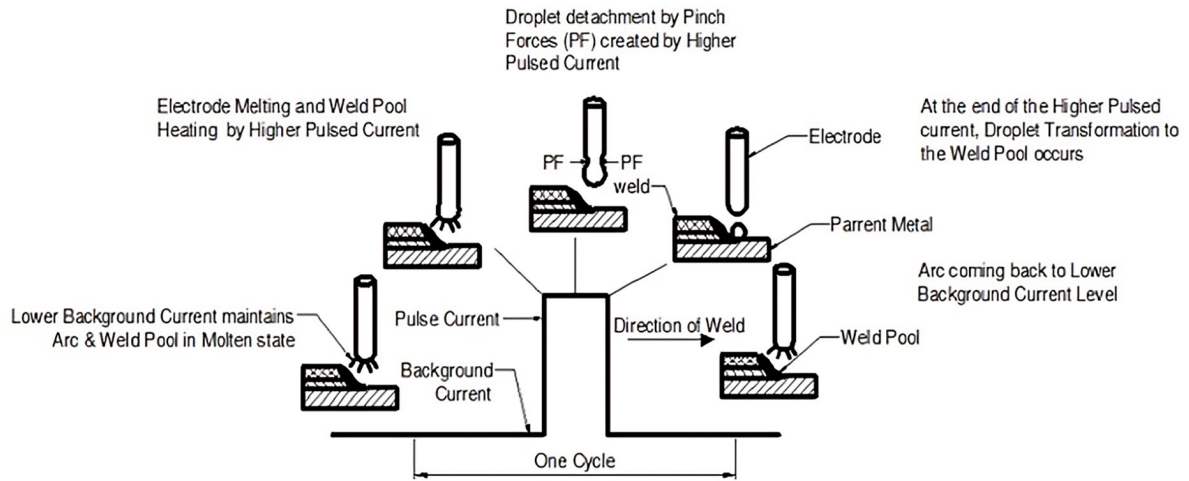


Figure 2: Metal transfer mechanism in PC-GMAW.

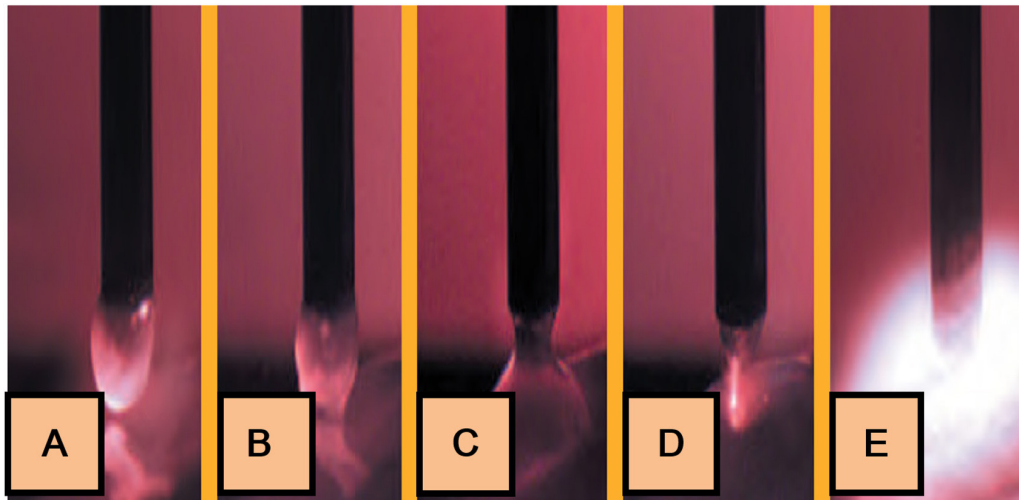


Figure 3: The various stages of FCAW under STT mode.

Table 2: Welding parameters for constant current – FCAW mode.

WELDING PARAMETERS	VALUES
Current (Amps)	164.5
Voltage (V)	23.1
Wire Feed Rate (inch/min)	252
Welding Speed (mm/sec)	4.18
Heat Input (kJ/mm)	0.9284

minimum of 10 seconds. The indent and the area of indentation are used to measure the hardness of the welded zone and HAZ by optically calculating the diagonal lengths of the left impression and are converted to HV by formula. The sample thickness is typically maintained at ten times the depth of indentation. The HV5 and HV10 methods are followed for stainless steel welding. The microhardness was carried out by using the Shimadzu/Newage HMV-2 Digital Micro-Hardness Tester. The welded specimens' surfaces were prepared for microscopic analysis by ASTM E3 standard. First, the surface was prepared using abrasive papers with varying grit sizes. Next, an alumina solution was used to polish the surface. Subsequently, Keller's reagent (ASTM E407) was used to etch the surfaces.

Table 3: Welding parameters for pulsed current – FCAW mode.

WELDING PARAMETERS	UNITS	NOTATION	ORIGINAL		
			LOW	MEDIUM	HIGH
Pulsed Current	Amps	A	190	210	230
Base Current	Amps	B	130	135	140
Frequency	Hz	C	80	100	120
Pulse on Time	%	D	40	60	80

Table 4: Welding parameters for pulsed current – FCAW mode.

PARAMETER/ FACTORS	UNITS	NOTATION	LEVELS		
			ORIGINAL		
			LOW	MEDIUM	HIGH
Background Current	Amps	A	75	85	95
Wire Feed Rate	m/min	B	4	4.4	4.8
Peak Current	Amps	C	200	220	240
Tail out	%	D	3	4	5

3. RESULTS AND DISCUSSION

3.1. Tensile behavior

The tensile strength results were obtained for both the base metal and the weld metal. The specimens used were of two categories for tensile strength testing, namely smooth surface specimen and notched surface specimen type for detailed insight into the fracture mechanics of the weldment [28]. Tensile properties with higher values were the desired outcome for the specimen in this analysis. The results of the tensile test are tabulated in Table 5. As can be inferred from the table, the yield strength and ultimate strengths are notably higher in the case of CC mode FCAW specimen in the case of smooth specimen followed by STT mode and PC mode specimens. This is the result of a high cooling rate induced during low heat input conditions that results in finer grain structure. The other reason is at low heat input due to the higher cooling rate, more ferrite is formed which is stronger between the two phases of DSS, thus improving the strength of the weldment. The increase in inter-pass temperature thereby promotes the increase of yield strength value in the weldment. This is the result of the formation of hard, brittle inter-metallic phases causing embrittlement [29].

In the case of the notched specimen, the yield and ultimate strength values peak for the PC mode specimen followed by STT mode and CC mode. However, an increase in the ductility of the joint was observed, indicated by the increased % elongation values. The graphs correlating the Yield and Tensile strengths of the smooth specimens and notched specimens are illustrated in Figures 4 and 5 respectively.

Figures 4–5 indicate that the weld metal strength is comparatively higher than that of the base metal; furthermore, the higher load capacity for fracture during tensile tests is also favorable for the weld metal about similar weld joints [30–31]. Yield strength is 781 KN in CC mode and in PC mode the yield strength is 568 KN and in STT mode the yield strength is 711KN which reveals that PC mode has a reduction of 31.5% in yield strength of DSS 2205 metal joints. The higher hardness induced due to welding is one of the reasons for experiencing higher strength in the DSS weldment. Likewise, the ultimate strength of the CC mode is greater than the PC mode and STT mode. This was due to the constant current supply of high heat energy more than the other two methods. This high heat energy melts the filler metal and gives a better joint of the materials. As the selected filler wire has strength higher than that of the base metal, it's clear that the strength of the weld metal is also higher and it is noted the fracture occurred well away from the weld metal. DSS weldment exhibits an almost similar strength in yield and ultimate tensile strength for all six samples that were tested. The test results show that the occurrence of fracture in the base metal (BM) is in the region as described in Table 5. The filler rod enriched with Nickel (ER 2209 grade) along with shielding gas is the contributor to the promotion of strength in the DSS weld. Moreover, all the test samples were fractured in the high-temperature HAZ region despite the said region possessing coarser ferrite grains. The tensile test results reveal the failure happening at a distance of 28.2 mm from the weld center which is present in BM. The UTS of the butt joint is the same as 705 MPa. The strength of the butt joint is 34% higher than that of the BM DSS 2205. The specimen has fractured with an angle

Table 5: Tensile properties of waveform-controlled FCAW – process.

FCAW MODE OF THE WELD	FRACTURE LOCATION	SMOOTH SPECIMEN						NOTCH SPECIMEN			STD DEV
		YS (MPa)	STD DEV	UTS (MPa)	STD DEV	% ELONGATION IN 25 mm GL	STD DEV	YS (MPa)	STD DEV	UTS (MPa)	
		MIN.-MAX.		MIN.-MAX.		MIN.-MAX.		MIN.-MAX.			
CC	Base	766–781	4.4	890–901	3.6	19–23	1.05	670–857	35.8	696–923	42.8
PC	Base	528–568	13.8	580–650	15.8	5–6	0.51	827–857	6.5	945–987	8.76
STT	Base	711–743	12.3	758–842	13.1	6–13	1.48	780–784	0.82	874–959	22.5

Yield and Tensile Strength - Smooth Specimens

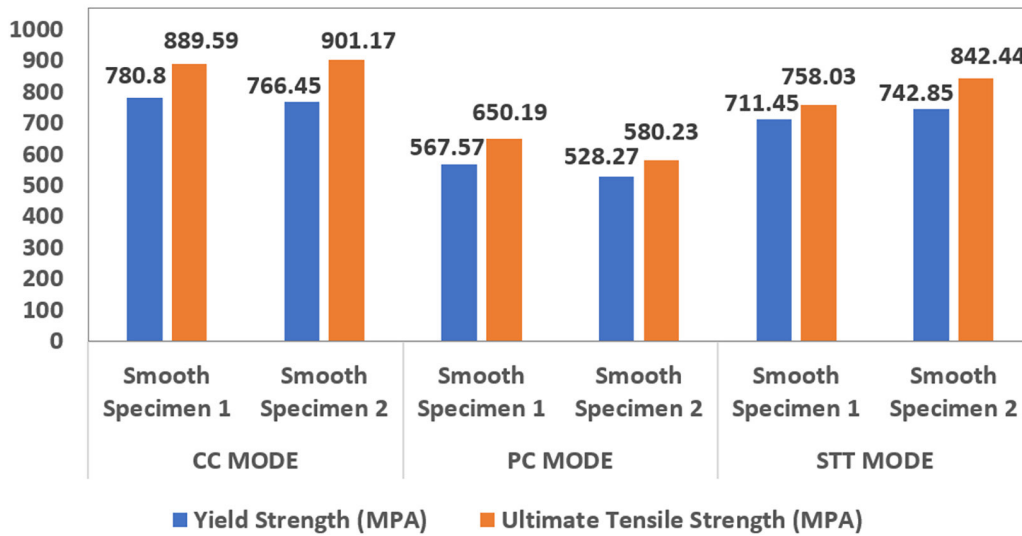


Figure 4: Yield and tensile strength of smooth specimens.

Yield and Tensile Strength - Notch Specimens

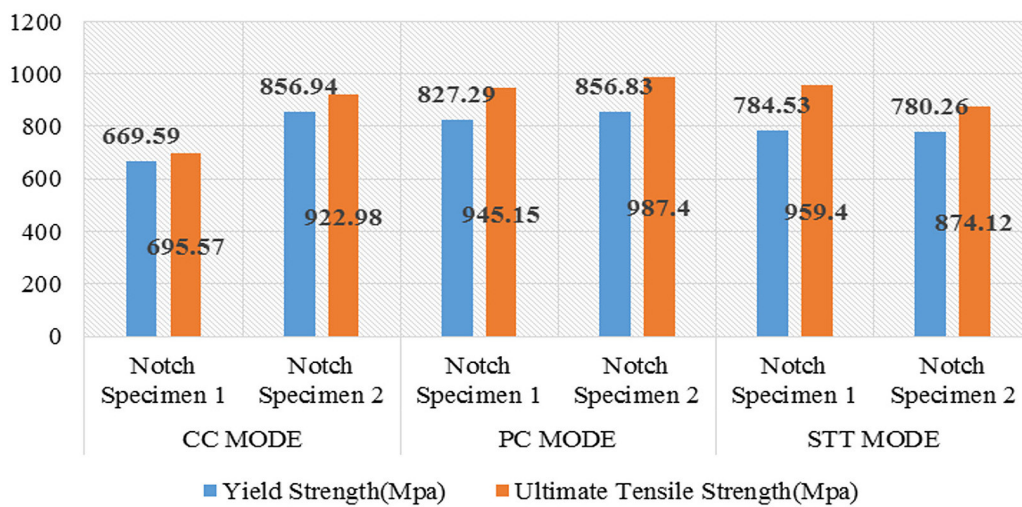


Figure 5: Yield and tensile strength of notch specimens.

of 45° orientations to the loading condition. The increased UTS of the butt weld is because of a greater quantity of hardness values at the FZ. Also, it enhances the fracture toughness and it results in the production of increased strength. The yield strength of the CC mode is larger when compared to the other two modes. Due to the variation in the percentage of elongation between the two phases of the material joined, after bending the weldment is shifted towards the DSS base metal side. More amount of plastic deformation was observed on the opposite notch side. All the test samples showed fractures happening outside of the weld region. The strength of the weld was found to be 5–10% higher in comparison to the BM [31, 32]. The filler wire used had higher strength than that of the base metal resulting in the fracture occurring well away from the weld metal. The strength obtained was at the peak at 842 MPa and 901 MPa for STT FCAW and CCFCAW respectively. There is no single mode that provides superior results for all the specimens.

As Table 5 reveals, for STT specimens in the cases of smooth and notched specimen types, the yield strength and ultimate strength values are relatively similar in comparison with the CC and PC modes whose values are hugely influenced by the specimen geometry. The percentage of elongation offered by the STT specimen also is in the middle ground in comparison to the types. The pulsed current and STT modes assure better performance in terms of mechanical strength with notch specimens. The STT mode and CC modes provide better results in the case of smooth specimens. Overall, the STT mode FCAW provides desirable results without loss of any major mechanical properties and is better suited for high-strength mechanical applications

3.2. Impact properties

Impact strength analysis is done for the specimens under the three FCAW conditions; CC, PC, and STT modes. The tests are used to analyze the toughness of the specimen to the energy absorption properties during plastic deformation. The impact strength of a material is analogous to the tensile strength of the material thereby the impact strength analysis could further validate the tensile strength analysis of a material. The test for impact strength was the Charpy impact test. The specimens were prepared for the impact test following standard ASTM procedures and were tested. The results obtained from the Charpy impact toughness test are tabulated in Table 6.

The results reveal impact strength for the base metal 58 J at room temperature of 24°C. This is taken as the reference point in comparison with the results of the specimens. The specimen was thick enough to ensure a high degree of plane strain loading; triaxiality over all the notched cross sections provided severe brittle fracture tests. The impact test measures the energy absorbed in the specimen's fracture. As the results in Table 6 postulate, the energy absorption rate of the specimens is higher in HAZ than in WZ. Hence the HAZ is more ductile than WZ. In CC mode the impact strength is more in the HAZ than the WZ, which is also the case for the PC mode specimen. Compared to CC mode, the energy absorption in PC mode is more in the weld metal and HAZ [33]. Hence, PC mode FCAW makes the metal weld more ductile than that of CC. The absorbed energy in HAZ of PC mode FCAW is 17.64% more than that of CC mode FCAW. A similar behavior is observed in STT mode just like CC and PC modes of FCAW. That is, more energy is absorbed in HAZ than in the weld metal. The energy absorbed in HAZ of STT is 52.3% more than that of CC and 42.07% more than PC modes of FCAW. Thus, the energy absorption is higher in the case of STT mode FCAW than that of PC and CC modes of FCAW. It implies that the weld made by STT mode is more ductile and will not show any embrittlement at the same temperatures used with the other two modes. In terms of Charpy impact test results, STT mode shows a better performance.

3.3. Fractographic analysis of tensile strength

Fractographic analysis of the Flux Core Arc Welded (FCAW) Duplex Stainless Steel (DSS) samples was conducted using scanning electron microscopy (SEM) to evaluate fracture modes in smooth tensile, notch tensile, and impact tests. The analysis revealed significant insights into the mechanical characteristics of the welds

Table 6: Impact test results for the modes CC, PC, and STT.

FCAW MODE OF THE WELD	IMPACT STRENGTH IN JOULES (58 J FOR BASE METAL AT 20° C)							
	WELD METAL			STD DEV	HAZ			STD DEV
	MIN.	MAX.	AVG.		MIN.	MAX.	AVG.	
CC	20	28	24	2.64	26	30	28	2.10
PC	24	38	31	4.44	26	42	34	5.16
STT	47	48	48	0.31	50	74	59	6.63

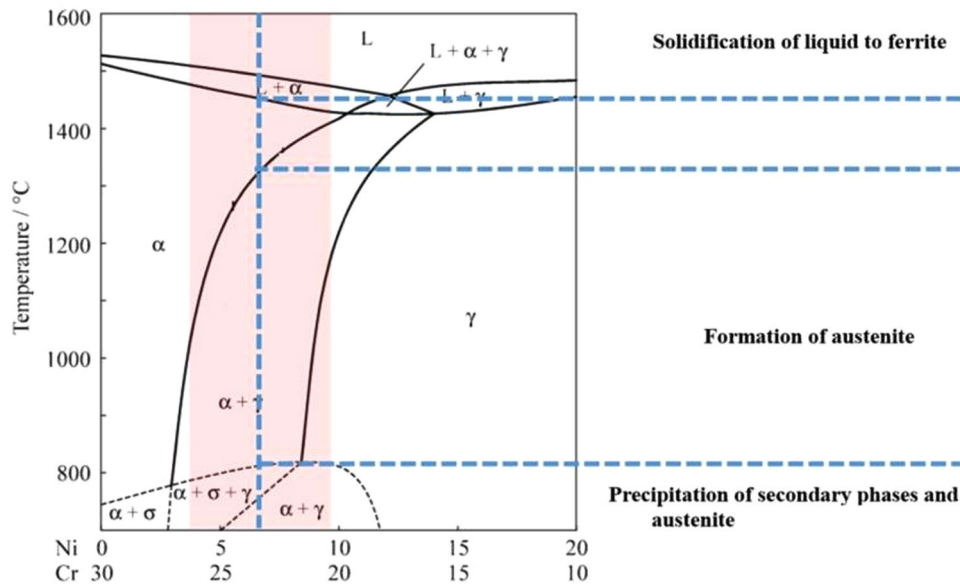


Figure 6: Phase diagram for 70% wt % of Fe in Fe-Cr-Ni. DPSS is illustrated as the shaded area in the above composition.

across different welding modes: Continuous Current (CC), Pulsed Current (PC), and Surface Tension Transfer (STT). From Figure 6 the phase diagram it is clear that the temperatures and compositions well beyond the shaded area result in secondary phases of the austenite phase. When the temperature is well below the shaded area it results in the alpha phase and above the temperature results in the gamma phase [34].

The results obtained for the STT mode of the FCAW SEM image are shown in Figures 7 and 8. When the same surface is welded through STT mode and when the HAZ zone near the smooth and notched specimens was measured, we could observe the increase in surface roughness and thereby due to the excess heating at the metal surface the grain growth could be observed which results in craters on the surfaces [17]. For welds produced using STT mode, the SEM images (Figures 7 and 8) show a uniform surface behavior with minimal abnormal grain growth or visible cracks. The STT mode exhibited a ductile fracture mode, characterized by a high density of dimples, indicating substantial plastic deformation before fracture [22]. Increased ductility and reduced fracture tendency have been known to be achieved through proper phase equilibrium and heat treatment. In contrast, welds created with high heat input have been found to exhibit more brittle characteristics, with notable intergranular cracking [23].

Smooth and notch tensile test Fractography images of STT FCAW are shown in Figures 7 and 8. The scanning electronic microscopic images show uniform surface behavior which is quite similar to that of the weldment surface and no such big craters or cracks could be observed on the surface. It is further surmised that the presence of higher delta ferrite content when high heat input during weld deposit leads to surface fracture. This shows a relatively smaller number of dimples in the fracture surface than those seen in low heat input welds. The high-volume fracture of dimples present at low heat input is significant in improving the strength of the weld joint as shown in Figures 7 and 8. The figures also highlight the effects of heat input on fracture behavior. High heat input conditions, such as those seen with CC mode, result in increased surface roughness and the formation of craters, indicative of significant grain growth and potential embrittlement [26], wherein elevated heat input could reduce fracture toughness and alter microstructural characteristics. The phase transitions occurring due to varying heat inputs affect fracture mechanisms, with high heat input promoting secondary phase formation, such as austenite, which can impact fracture behavior. Rapid cooling and subsequent phase transformations have been known to influence the fracture mode and overall ductility [28].

As can be observed from Figure 9, The irregular isolation of alloying elements and the formation of the elements constituting secondary austenite and ferrite phases lead to the ductile-brittle transition of DSS welds at lower temperatures [35, 36]. The coarser the ferrite grains, the nearer the fusion boundaries occur, constituting low-impact energy. When compared with the obtained results of fractographic analysis for the STT mode of FCAW, it could well prove that the surface possesses uniformity and that no abnormal grain growth could be observed nor the cracks in the pattern could be visualized. The transition from ductile to brittle fracture modes is influenced by temperature and phase composition. An increase in temperature generally leads to more ductile

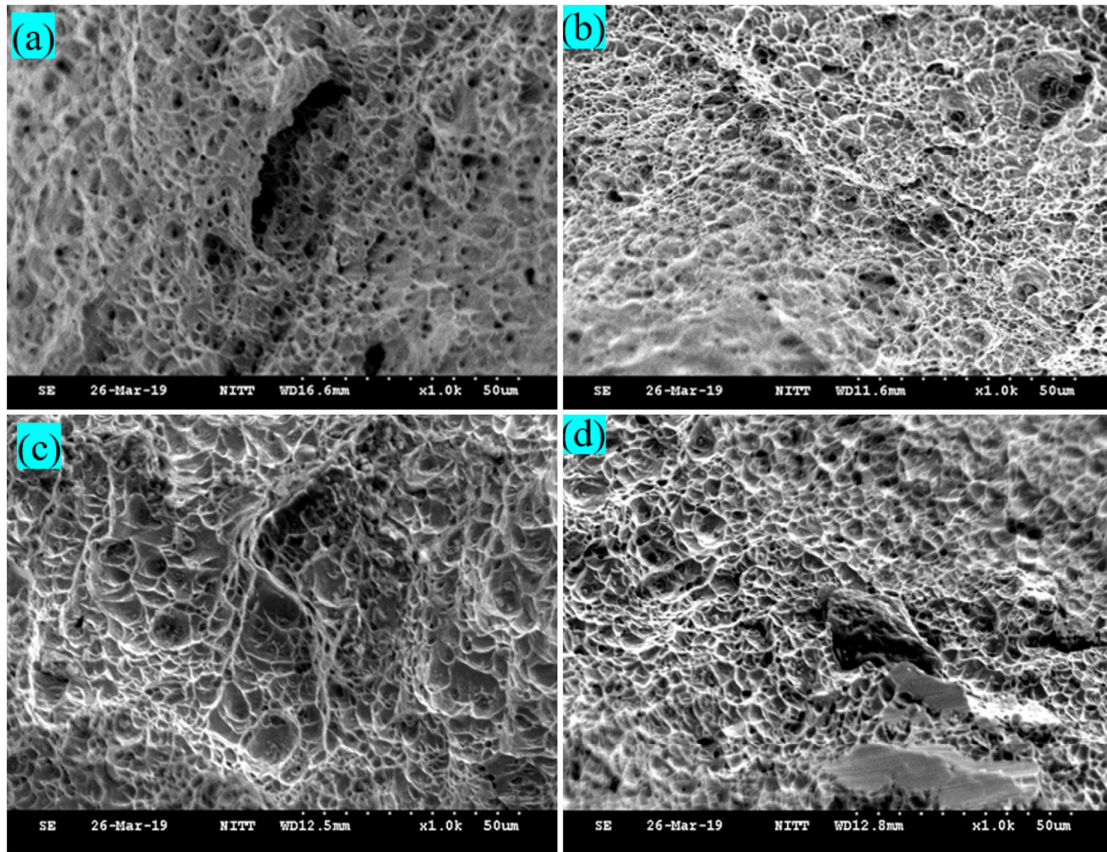


Figure 7: Fractographical analyses by tensile test smooth specimen (a) base metal (b) Weld (c) HAZ and (d) TMAZ of welded samples.

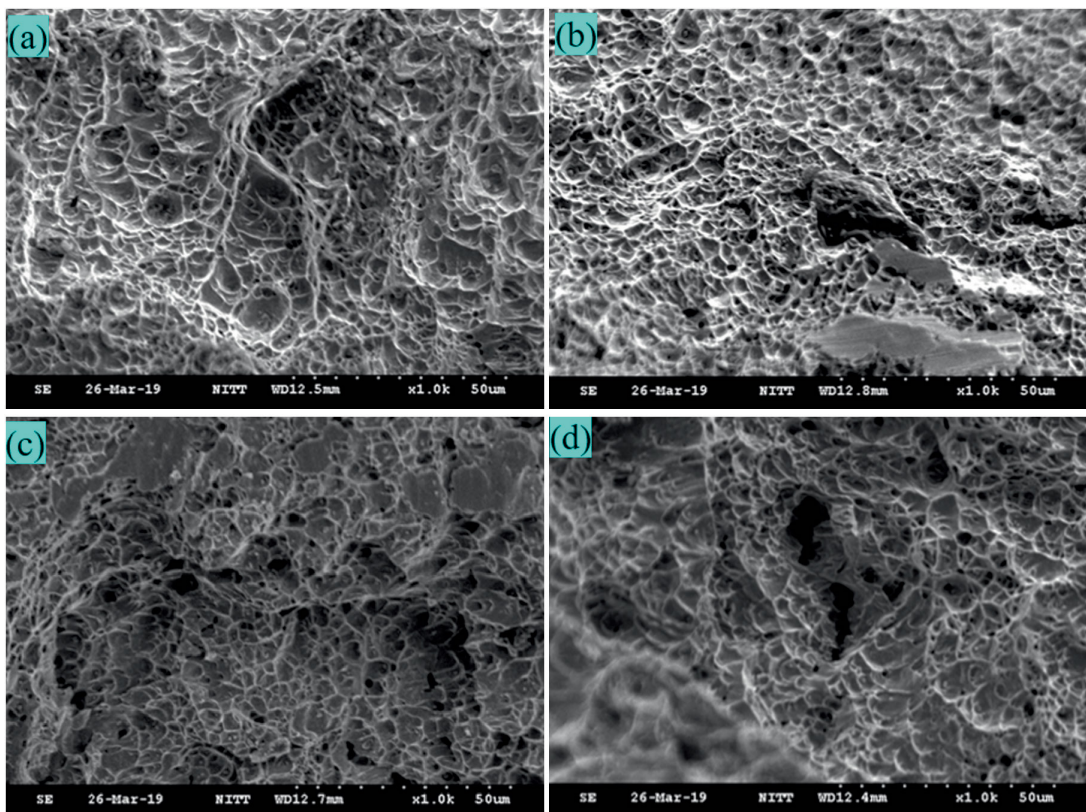


Figure 8: Fractographical analyses by tensile test notched specimen (a) base metal (b) Weld (c) HAZ and (d) TMAZ of welded samples.

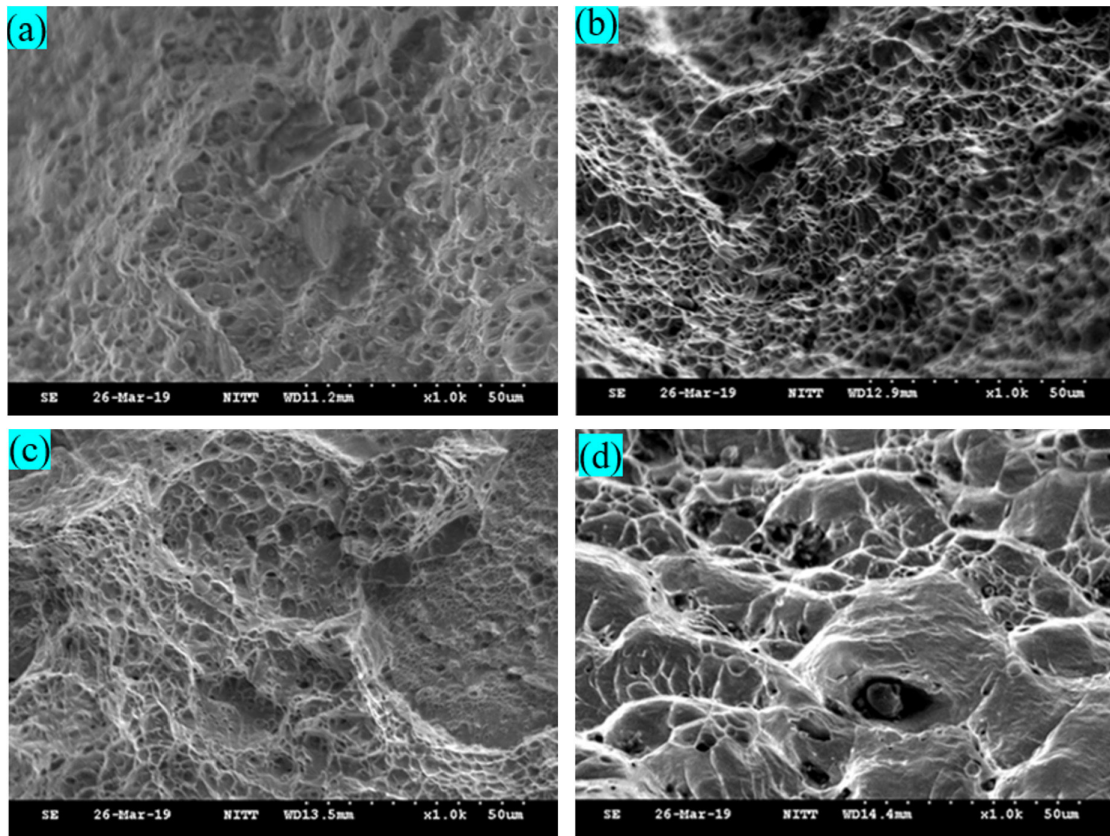


Figure 9: Fractographical analysis by impact test (a) base metal (b) welded (c) HAZ and (d) TMAZ of welded samples.

behavior, whereas lower temperatures result in brittle fractures. This indicates the need for controlling welding parameters to achieve optimal fracture toughness and mechanical performance [37, 38].

3.4. Hardness analysis

The hardness analysis was carried out for the FCA welded specimen of three weld modes. The Vickers hardness analysis was followed for the characterization of the microhardness properties of the specimens for the characterization of the material's strength [17]. This hardness test of welding is intended to assess the strength of the welding, largely to get the hardness near the heat-affected zone (HAZ). The hardness surrounding the heat-affected region governs the brittleness/flimsiness of the weld. The hardness values are indicated in terms of Vickers number with the notation "HV". The Vickers hardness is achieved with the help of the applied load to the indent and the area of indentation. The applied load ranges from 10 gf to 100 kgf. For micro-hardness testing, the load is normally less than or equal to 1 kgf. The surface of the sample is polished before this test either mechanically or by electrical means. The procedure followed to conduct this test is as per ASTM E384 standard. The maximum time of indentation is 15 seconds and the minimum should not be less than 10 seconds. The sample thickness is typically maintained at ten times the depth of indentation. The HV5 and HV10 methods are followed for stainless steel welding. The measurements are made in series at a certain distance from the verge of the sample or topmost of the weld. The hardness values are tabulated in Table 7. Graphical representations of hardness values for each FCAW mode specimen are represented in Figures 10–12. A comparison chart in Figure 13 provides insight into the faring of the specimens in hardness properties.

The Vickers hardness value for the base metal specimen was found to be 282.23 HV. This hardness value is considered as a reference point for the subsequent hardness analysis of the specimens, and their values are compared in Table 7.

3.4.1. Hardness analysis of CC mode FCAW specimen

As inferred from Table 7, the hardness value obtained in the HAZ of the CC mode specimen is found to be 282.47 HV. The hardness on the WZ was obtained as 280.24 HV. Concurrently, the hardness value from LT HAZ near BM was higher than the BM value; HT HAZ near the WZ had a hardness similar to the base metal

Table 7: Vickers hardness values obtained at several zones of DSS 2025 with FCAW.

ZONE/REGION	FCAW – CONSTANT CURRENT (CC) MODE	FCAW – PULSED CURRENT (PC) MODE	FCAW – SURFACE TENSION TRANSFER (STT) MODE
Base Metal	282.23 VHN		
LT HAZ	285.97 VHN	291.9 VHN	296.7 VHN
Heat Affected Zone (HAZ)	282.47 VHN	287.69VHN	295.55VHN
HT HAZ	278.97 VHN	293.1 VHN	300.27 VHN
Welded Zone	280.24 VHN	307.69 VHN	293.9 VHN

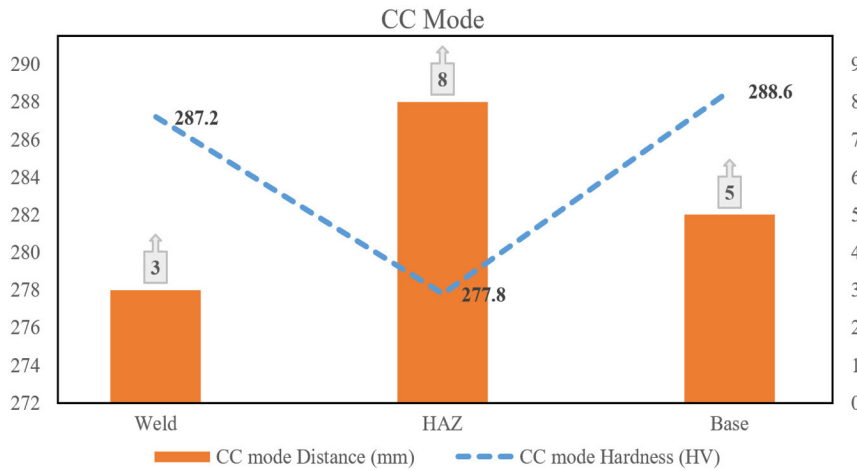


Figure 10: Hardness values and distance – CC mode.

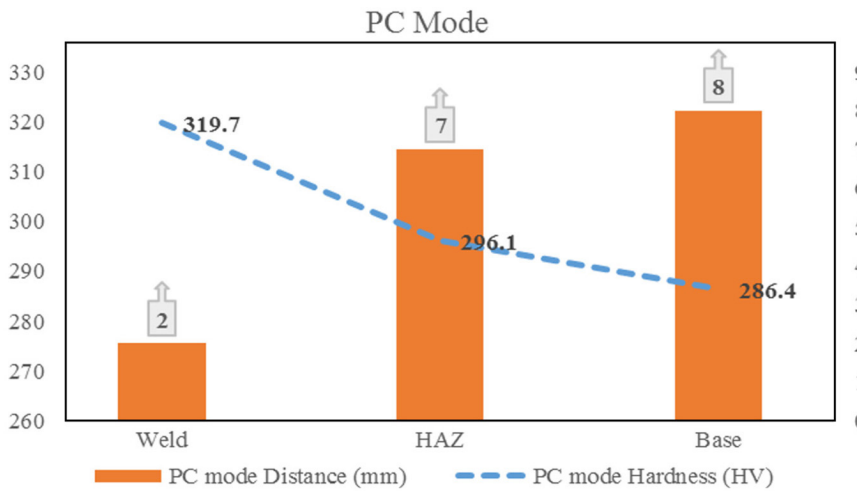


Figure 11: Hardness values and distance – PC mode.

hardness value. The hardness value obtained from the CC mode specimen was not much higher than the base metal hardness. This trend can be witnessed in Figure 10.

3.4.2. Hardness analysis of PC mode FCAW specimen

As inferred from Figure 11, the PC mode specimen hardness was tested at HAZ in low-temperature and high-temperature zones of the metal. The hardness values are shown in Table 7. These values correspond to the hardness value near the weldment; the hardness of WZ and HT HAZ are higher in comparison to BM, HAZ & LT HAZ respectively.

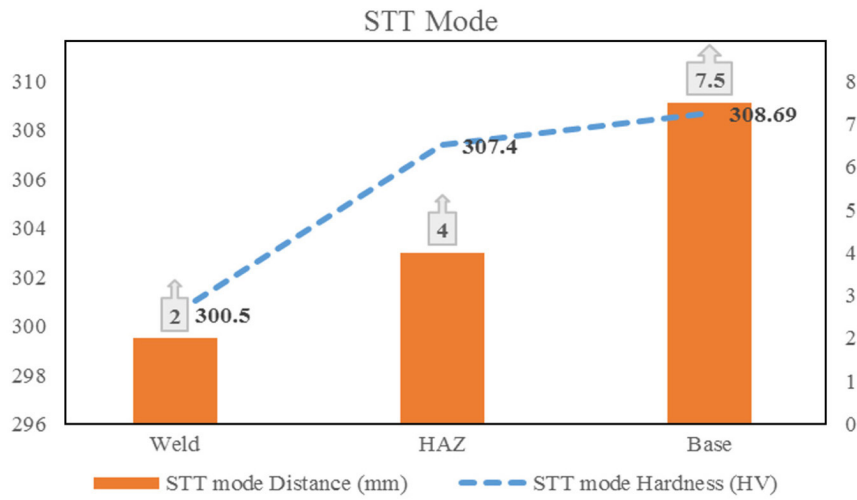


Figure 12: Hardness values and distance – STT mode.

Hardness at various regions at different modes of FCAW

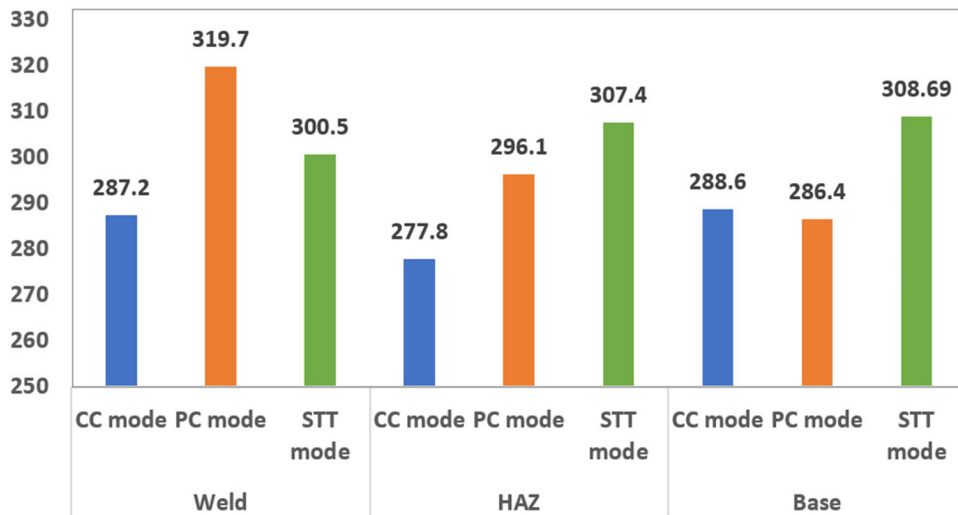


Figure 13: Comparisons of hardness values – various modes of FCAW.

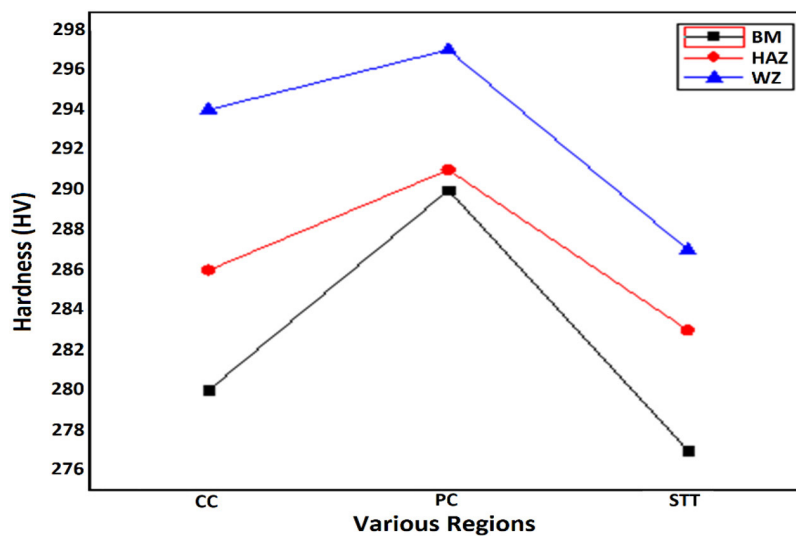


Figure 14: Hardness measurements for various weldments.

3.4.3. Hardness analysis of STT mode FCAW specimen

As observed from Figure 12, the STT mode specimen hardness was tested at HAZ in low-temperature and high-temperature zones of the metal. The values corresponding to the tested zones reveal the trend that the hardness of HT HAZ is greater than the LT HAZ followed by HAZ and WZ in that specific order. The reason for the hardness value being greater at that juncture could be attributed to the fact that this zone had uneven cooling between the zones.

The Vickers hardness analysis across different modes of Flux Core Arc Welding (FCAW) in Duplex Stainless Steel (DSS) reveals specific trends (Figures 12–14). In the Constant Current (CC) mode, the highest hardness values are observed near the base metal at LT HAZ, gradually decreasing towards the weld metal section. Pulsed Current (PC) mode shows maximum hardness predominantly in the weld metal, with lower values in the HAZ regions and the lowest values in the base metal. Surface Tension Transfer (STT) mode exhibits the highest hardness near the HT HAZ and base metal regions, indicating potential improvements in mechanical properties and reduced brittleness compared to CC and PC modes. These findings highlight the significant influence of heat input and cooling dynamics on microstructure and mechanical performance in DSS weldments under various FCAW conditions.

4. CONCLUSION

The mechanical properties of Flux Core Arc Welded (FCAW) Duplex Stainless Steel (DSS) were analyzed through the tests for mechanical strength such as the Tensile Test and Impact Test, Fractographical analysis, and Micro-Hardness Test (Vickers Hardness Test).

- Surface Tension Transfer (STT) mode Flux Core Arc Welding (FCAW) demonstrated superior mechanical properties in Duplex Stainless Steel (DSS) compared to Constant Current (CC) and Pulsed Current (PC) modes.
- Tensile strength tests showed higher yield and ultimate strengths in STT mode welds, indicating improved weld quality and mechanical integrity.
- Impact strength analysis revealed that STT mode welds absorbed the highest energy, suggesting enhanced ductility and resistance to brittle fracture.
- Fractographic analysis confirmed uniform surface properties and minimal defects in STT mode welds, underscoring their robustness.
- Vickers hardness testing indicated higher values in the Heat Affected Zone (HAZ) near the weldment for STT mode, highlighting superior strength characteristics.
- STT mode FCAW is recommended for achieving high-performance welds in DSS, suitable for industrial and structural applications requiring superior mechanical properties and weld integrity.
- Future research could explore additional parameters to further optimize and enhance the performance of STT mode FCAW in diverse welding applications.

5. REFERENCES

- [1] DAVIS, J.R., *Alloy Digest Sourcebook: Stainless Steels*, Materials Park, ASM International, 2000.
- [2] VON HOFE, D., *Significance of welding and joining technology in a modern industrial structure*, Ural Federal University, German welding society (DVS), Germany, Krefeld, 2015.
- [3] IBRAHIM, T., YAWAS, D.S., AKU, S.Y., “Effects of gas metal arc welding techniques on the mechanical properties of duplex stainless steel”, *Journal of Minerals & Materials Characterization & Engineering*, v. 1, n. 5, pp. 222–230, 2013. doi: <http://doi.org/10.4236/jmmce.2013.15035>.
- [4] PAL, K., PAL, S.K., “Effect of pulse parameters on weld quality in pulsed gas metal arc welding: a review”, *Journal of Materials Engineering and Performance*, v. 20, n. 6, pp. 918–931, 2011. doi: <http://doi.org/10.1007/s11665-010-9717-y>.
- [5] EGHLIMI, A., SHAMANIAN, M., RAEISSI, K., “Dilution and ferrite number prediction in pulsed current cladding of super duplex stainless steel using RSM”, *Journal of Materials Engineering and Performance*, v. 22, n. 12, pp. 3657–3664, 2013. doi: <http://doi.org/10.1007/s11665-013-0661-5>.
- [6] GRAJCAR, A., RÓŻAŃSKI, M., STANO, S., *et al.*, “Effect of heat input on microstructure and hardness distribution of laser welded Si-Al TRIP-type steel”, *Advances in Materials Science and Engineering*, v. 2014, n. 1, pp. 1–8, 2014. doi: <http://doi.org/10.1155/2014/658947>.

- [7] HIRATA, Y., “Pulsed arc welding”, *Welding International*, v. 17, n. 2, pp. 98–115, 2003. doi: <http://doi.org/10.1533/wint.2003.3075>.
- [8] LINCOLN ELECTRIC COMPANY, *Surface Tension Transfer STT Waveform Control Technologies*, PRRE Welding Technology, Josink Esweg 43, 7545PN Enschede, 2017.
- [9] CHAGAS DE SOUZA, G., DA SILVA, A.L., TAVARES, S.S.M., *et al.*, “Mechanical properties and corrosion resistance evaluation of super duplex stainless steel UNS32760 repaired by GTAW process”, *Welding International*, v. 30, n. 6, pp. 432–442, 2016. doi: <http://doi.org/10.1080/09507116.2015.1096527>.
- [10] MUTHUSAMY, C., KARUPPIAH, L., PAULRAJ, S., *et al.*, “Effect of heat input on mechanical and metallurgical properties of gas tungsten arc welded lean super martensitic stainless steel”, *Materials Research*, v. 19, n. 3, pp. 572–579, 2016. doi: <http://doi.org/10.1590/1980-5373-MR-2015-0538>.
- [11] ESMAILZADEH, M., SHAMANIAN, M., KERMANPUR, A., *et al.*, “Microstructure and mechanical properties of friction stir welded lean duplex stainless steel”, *Materials Science and Engineering A*, v. 561, pp. 486–491, 2013. doi: <http://doi.org/10.1016/j.msea.2012.10.068>.
- [12] DONG, H., HAO, X., DENG, D., “Effect of welding heat input on microstructure and mechanical properties of HSLA steel joint”, *Metallography, Microstructure, and Analysis*, v. 3, n. 2, pp. 138–146, 2014. doi: <http://doi.org/10.1007/s13632-014-0130-z>.
- [13] HOSSEINI, V.A., BERMEJO, M.A.V., GÅRDSTAM, J., “Influence of multiple thermal cycles on microstructure of heat-affected zone in tig-welded super duplex stainless steel”, *Welding in the World*, v. 60, n. 2, pp. 233–245, 2016. doi: <http://doi.org/10.1007/s40194-016-0300-5>.
- [14] IBRAHIM, O., IBRAHIM, I., KHALIFA, T., “Impact behavior of different stainless-steel weldments at low temperatures”, *Engineering Failure Analysis*, v. 17, n. 5, pp. 1069–1076, 2010. doi: <http://doi.org/10.1016/j.engfailanal.2009.12.006>.
- [15] ŁABANOWSKI, J., “Mechanical properties and corrosion resistance of dissimilar stainless-steel welds”, *Archives of Materials Science and Engineering*, v. 28, n. 1, pp. 27–33, 2007.
- [16] LI, L., CHAI, M., LI, Y., *et al.*, “Effect of welding heat input on grain size and microstructure of 316L stainless steel welded joint”, *Applied Mechanics and Materials*, v. 331, pp. 578–582, 2013. doi: <http://doi.org/10.4028/www.scientific.net/AMM.331.578>.
- [17] ZHANG, Z., JING, H., XU, L., *et al.*, “Influence of heat input in electron beam process on microstructure and properties of duplex stainless-steel welded interface”, *Applied Surface Science*, v. 435, pp. 352–366, 2018. doi: <http://doi.org/10.1016/j.apsusc.2017.11.125>.
- [18] MOSA, E.S., MORSY, M.A., ATLAM, A., “Effect of heat input and shielding gas on microstructure and mechanical properties of austenitic stainless steel 304L”, *International Research Journal of Engineering and Technology*, v. 4, n. 12, pp. 370–377, 2017.
- [19] KANGAZIAN, J., SHAMANIAN, M., “Effect of pulsed current on the microstructure, mechanical properties and corrosion behavior of ni-based alloy/super duplex stainless steel dissimilar welds”, *Transactions of the Indian Institute of Metals*, v. 72, n. 9, pp. 2403–2416, 2019. doi: <http://doi.org/10.1007/s12666-019-01693-1>.
- [20] KANGAZIAN, J., SHAMANIAN, M., “Mechanical and microstructural evaluation of SAF 2507 and Incoloy 825 dissimilar welds”, *Journal of Manufacturing Processes*, v. 26, pp. 407–418, 2017. doi: <http://doi.org/10.1016/j.jmapro.2017.03.006>.
- [21] SHAMANIAN, M., KANGAZIAN, J., SZPUNAR, J.A., “Insights into the microstructure evolution and crystallographic texture of API X-65 steel/UNS S32750 stainless steel dissimilar welds by EBSD analysis”, *Welding in the World*, v. 65, n. 5, pp. 973–986, 2021. doi: <http://doi.org/10.1007/s40194-020-01062-3>.
- [22] SABZI, M., DEZFULI, S.M., “Drastic improvement in mechanical properties and weldability of 316L stainless steel weld joints by using electromagnetic vibration during GTAW process”, *Journal of Manufacturing Processes*, v. 33, pp. 74–85, 2018. doi: <http://doi.org/10.1016/j.jmapro.2018.05.002>.
- [23] SABZI, M., ANIJDAN, S.H.M., CHALANDAR, A.R.B., *et al.*, “An experimental investigation on the effect of gas tungsten arc welding current modes upon the microstructure, mechanical, and fractography properties of welded joints of two grades of AISI 316L and AISI 310S alloy metal sheets”, *Materials Science and Engineering A*, v. 840, pp. 142877, 2022. doi: <http://doi.org/10.1016/j.msea.2022.142877>.
- [24] SABZI, M., ANIJDAN, S.H.M., EIVANI, A.R., *et al.*, “The effect of pulse current changes in PCGTAW on microstructural evolution, drastic improvement in mechanical properties, and fracture mode of dissimilar

- welded joint of AISI 316L-AISI 310S stainless steels”, *Materials Science and Engineering A*, v. 823, pp. 141700, 2021. doi: <http://doi.org/10.1016/j.msea.2021.141700>.
- [25] TABRIZI, T.R., SABZI, M., ANIJ DAN, S.H.M., *et al.*, “Comparing the effect of continuous and pulsed current in the GTAW process of AISI 316L stainless steel welded joint: microstructural evolution, phase equilibrium, mechanical properties and fracture mode”, *Journal of Materials Research and Technology*, v. 15, pp. 199–212, 2021. doi: <http://doi.org/10.1016/j.jmrt.2021.07.154>.
- [26] ANIJ DAN, S.H., SABZI, M., GHOBEITI-HASAB, M., *et al.*, “Optimization of spot welding process parameters in dissimilar joint of dual phase steel DP600 and AISI 304 stainless steel to achieve the highest level of shear-tensile strength”, *Materials Science and Engineering A*, v. 726, pp. 120–125, 2018. doi: <http://doi.org/10.1016/j.msea.2018.04.072>.
- [27] SABZI, M., DEZFULI, S.M., “Post weld heat treatment of hypereutectoid Hadfield steel: Characterization and control of microstructure, phase equilibrium, mechanical properties and fracture mode of welding joint”, *Journal of Manufacturing Processes*, v. 34, pp. 313–328, 2018. doi: <http://doi.org/10.1016/j.jmapro.2018.06.009>.
- [28] ANIJ DAN, S.H.M., SABZI, M., “The Effect of heat treatment process parameters on mechanical properties, precipitation, fatigue life, and fracture mode of an austenitic mn hadfield steel”, *Journal of Materials Engineering and Performance*, v. 27, n. 10, pp. 5246–5253, 2018. doi: <http://doi.org/10.1007/s11665-018-3625-y>.
- [29] SABZI, M., OBEYDAVI, A., ANIJ DAN, S.H.M., “The effect of joint shape geometry on the microstructural evolution, fracture toughness, and corrosion behavior of the welded joints of a Hadfield Steel”, *Mechanics of Advanced Materials and Structures*, v. 26, n. 12, pp. 1053–1063, 2018. doi: <http://doi.org/10.1080/15376494.2018.1430268>.
- [30] JAFARIAN, H.R., SABZI, M., ANIJ DAN, S.H.M., *et al.*, “The influence of austenitization temperature on microstructural developments, mechanical properties, fracture mode and wear mechanism of Hadfield high manganese steel”, *Journal of Materials Research and Technology*, v. 10, pp. 819–831, 2021. doi: <http://doi.org/10.1016/j.jmrt.2020.12.003>.
- [31] AGUIRRE, H.V.M., TEIXEIRA, F.R., MOTA, C.A.M.D., *et al.*, “Evaluation of dissimilar welds with the double-layer technique using AWS ER 316L and ER NiCrMo-3 electrode wires on ASTM A182 F22 steel”, *Matéria (Rio de Janeiro)*, v. 26, pp. e13000, 2021. doi: <http://doi.org/10.1590/s1517-707620210003.13000>.
- [32] SILVA, P.P.B.D., ARAÚJO, I.D.S., VIEIRA, M.R.S., *et al.*, “Influence of welding parameters on the geometric and microstructural characteristics of Inconel 625 coatings deposited on ASTM A36 Steel by Plasma Transferred Arc”, *Matéria (Rio de Janeiro)*, v. 25, n. 2, pp. e12650, 2020. doi: <http://doi.org/10.1590/s1517-707620200002.1050>.
- [33] ALVARÃES, C.P., MADALENA, F.C.A., SOUZA, L.F.G.D., *et al.*, “Performance of the INCONEL 625 alloy weld overlay obtained by FCAW process”, *Matéria (Rio de Janeiro)*, v. 24, n. 1, pp. e12290, 2019. doi: <http://doi.org/10.1590/s1517-707620190001.0627>.
- [34] GIAROLLO, D.F., MAZZAFERRO, C.C.P., MAZZAFERRO, J.A.E., “Effect of filler material on sliding wear resistance of a structural steel welded by GMAW”, *Matéria (Rio de Janeiro)*, v. 24, pp. e12464, 2019. doi: <http://doi.org/10.1590/s1517-707620190003.0780>.
- [35] ZAPPA, S., PÉREZ, H., SVOBODA, H., *et al.*, “Characterization of corrosion behavior in superduplex stainless steel overburden welds”, *Matéria (Rio de Janeiro)*, v. 23, pp. e12014, 2018.
- [36] SILVA, C.M.D., CUNHA, T.V.D., MIKOWSKI, A., “Mechanical and microstructural analysis of welds produced by the submerged arc process with ultrasonic pulsation of the current”, *Matéria (Rio de Janeiro)*, v. 22, n. 4, pp. e11896, 2017.
- [37] SOUZA, D.D.B.G.D., FERRARESI, V.A., “Application of hardfacing of different types consumables used in sucroal-cooleira industry with the FCAW double wire process”, *Matéria (Rio de Janeiro)*, v. 22, pp. e11794, 2017.
- [38] BRANDIM, A.S., MAGALHÃES SOUSA, R.R., ROCHA PARANHOS, R.P., *et al.*, “Microstructure evolution of 423Co martensitic stainless steel coatings under thermal fatigue tests”, *Matéria (Rio de Janeiro)*, v. 16, pp. 714–729, 2011. doi: <http://doi.org/10.1590/S1517-70762011000200007>.